Journal of Statistical Physics, Vol. 104, Nos. 1/2, 2001

Continuum Theory of Epitaxial Crystal Growth. I

Weinan E[1] **and Nung Kwan Yip**[2]

Received February 14, 2000; revised February 6, 2001

We present various continuum limits to describe epitaxial thin film growth. We consider a hierarchy of models which can take into account the diffusion of terrace adatoms, attachment and detachment of edge adatoms, vapor phase diffusion and the effect of multiple species. The starting point is the Burton–Cabrera–Frank type step flow model. We have obtained partial differential equations in the form of a coupled system of diffusion equation for the adatom density and a Hamilton–Jacobi equation for the film height function. This is supplemented with appropriate boundary conditions at the continuum level to describe the growth at the peaks and valleys on the film. The results here can be used in a macroscopic description of thin film growth.

KEY WORDS: Epitaxial growth; Burton–Cabrera–Frank (BCF) step flow model; continuum limit.

1. INTRODUCTION

The purpose of the present paper is to derive continuum limits of step flow models used in the study of crystal growth. We are mainly interested in the regime where the growth is *epitaxial*, i.e., layer by layer growth of a crystalline thin film on a suitably chosen substrate. The atomic and lattice structures play important role in these growth processes. This is in contrast with the Mullins–Sekerka type of models which are typically applicable to amorphous solids or growth from the liquid phase.(12, 14, 15, 17) The simplest example of interest is found in *molecular beam epitaxy* (MBE)(25) in which adatoms are delivered under ultra-high vacuum conditions onto the surface where they diffuse until they are incorporated at a step or other surface defects. Other more complicated growth methods such as *chemical vapor*

---

[1] Department of Mathematics and Program in Applied and Computational Mathematics, Princeton University, Courant Institute, New York University.

[2] Department of Mathematics, Purdue University.

0022-4715/01/0700-0221$19.50/0

deposition (CVD) can also achieve the kind of epitaxial growth described by the step flow models studied in this paper.

The foundation for the theory of crystal growth was laid out in the paper of Burton, Cabrera and Frank (BCF).(2) It is also the starting point of the present work. Recognizing that the vapor-solid interface consists of three different kinds of geometric objects—*terraces*, *steps* and *kinks* of dimensions *two, one* and *zero* respectively—BCF postulates that atoms in the vapor phase land on the terraces and then diffuse until they meet a step along which they continue to diffuse until they are finally incorporated into the kink sites along the steps (Fig. 1). The diffusing atoms on the interface are called *adatoms*. The original BCF theory concentrates on diffusion on the terraces. The paper of Caflisch *et al.*(4) extends this theory to the full *terrace-step-kink* hierarchy. Modern account of the theory of crystal growth can be found in refs. 6 and 18.

At the atomic scale, the growth of a crystal should be described by the hopping of adatoms between different lattice sites on the interface. The kinetic monte carlo (KMC) or solid on solid (SOS) models operate at this level.(22) BCF type of theory operates at the next level where the terraces are treated as a continuum and the crystal grows as a result of the steps moving in the horizontal direction. Our principal objective is to develop a theory that operates at an even larger scale at which the interface is described by a continuous height function and is seen to consist of mountain peaks and valleys. In principle, we can go to an even larger scale over which many peaks and valleys are homogenized. But we will not do so in this paper.

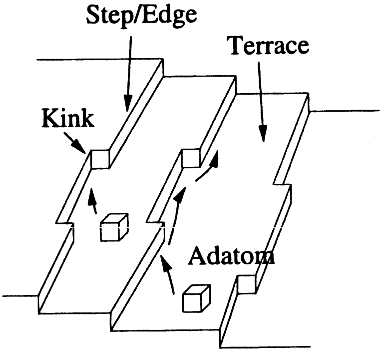

Fig. 1. A two dimensional crystal surface can be described by the Terrace–Step(Ledge)–Kink model.

There is an abundance of continuum equations in the literature describing epitaxial growth.(7, 10, 26, 27) Most of these equations take the form of a fourth order partial differential equations for the thin film height function. Our work is different in two aspects. Firstly, we strive to derive these equations rigorously from step flow models instead of posing them on phenomenological grounds. Secondly and more importantly, the equations we obtain form a *coupled system* for both the *height function* and the *adatom densities*. This is crucial if surface chemistry is going to be incorporated in the growth models.

This paper is organized as follows. In the next section, we present the BCF step flow model and its generalizations. In Section 3, we derive two continuum limits for vicinal surfaces. In Section 4, we discuss boundary conditions at mountain peaks and valleys. These three sections are the core of the present paper. Then we extend our model to $2+1$ dimensions (Section 5) and also incorporate vapor phase diffusion (Section 6). The appendix includes some technical derivations and extensions.

2. BCF THEORY OF DIFFUSION AND ITS GENERALIZATIONS

2.1. BCF Theory

We will concentrate on the case of a single step. Extension to multiple steps is obvious. The description below is for $2+1$ dimensions.

Denote by $\Omega_-(t)$ and $\Omega_+(t)$ the upper and lower terraces separated by a step $\Gamma(t)$ (Fig. 2). Let ρ be the number density of adatoms on the terrace. Then ρ satisfies the following standard diffusion equation on the terraces $\Omega_-(t)$ and $\Omega_+(t)$:

$$\rho_t = D \triangle \rho - \frac{\rho}{\tau} + F \tag{1}$$

where F is the deposition flux; D is the diffusion constant on the terrace; τ is the evaporation time which is the average time that an adatom resides on the terrace without being incorporated at the steps. Denote also by $\mathbf{v}$ and $\mathbf{n}$ the velocity and normal vector of the step $\Gamma(t)$ pointing to the lower terrace.

To obtain the boundary conditions for (1) at $\Gamma(t)$, consider the following:

$$\begin{aligned}\frac{d}{dt}\int_{\Omega_-(t)} \rho\, dA &= \int_{\Omega_-(t)} \rho_t\, dA + \int_{\Gamma(t)} \rho(\mathbf{v}\cdot\mathbf{n})\, ds \\ &= \int_{\Gamma(t)} \left(D\frac{\partial \rho}{\partial n} + \rho \mathbf{v}\cdot\mathbf{n} \right) ds + \int_{\Omega_-(t)} \left(F - \frac{\rho}{\tau} \right) dA \end{aligned} \tag{2}$$

The first term on the right hand side of (2) represents the flux of adatoms from the upper terrace to the step $\Gamma(t)$ as a result of diffusion and step motion. Similarly, we have

$$\frac{d}{dt}\int_{\Omega_+(t)} \rho \, dA = -\int_{\Gamma(t)} \left(D\frac{\partial \rho}{\partial n} + \rho \mathbf{v}\cdot\mathbf{n} \right) ds + \int_{\Omega_+(t)} \left(F - \frac{\rho}{\tau} \right) dA \tag{3}$$

Now we need constitutive relations for these fluxes. It is natural to postulate the following type of *linear* kinetic relation:

$$J_+ = -\left(D\frac{\partial \rho}{\partial n} + \rho \mathbf{v}\cdot\mathbf{n} \right)\Big|_+ = \alpha_+(\rho - \rho_e) \tag{4}$$

$$J_- = \left(D\frac{\partial \rho}{\partial n} + \rho \mathbf{v}\cdot\mathbf{n} \right)\Big|_- = \alpha_-(\rho - \rho_e) \tag{5}$$

where ρ_e is the equilibrium adatom density at the step. Among other things, ρ_e may depend on the temperature as well as the geometric characteristic of the step $\Gamma(t)$ such as the curvature. The numbers α_+ and α_- are the *hopping rates* of adatoms to the step from the lower and upper terraces.

In the original paper of BCF, the adatom density at the step is assumed to be at its equilibrium value:

$$\rho^\pm = \rho_e. \tag{6}$$

An additional boundary condition comes as a consequence of the conservation of adatoms. Noting that adatoms on the steps are eventually

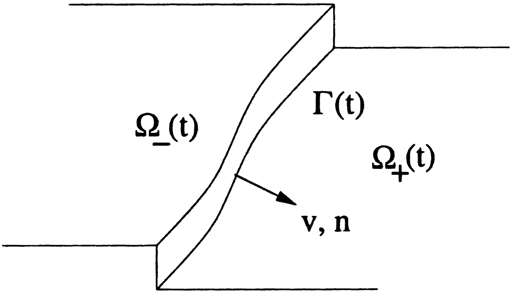

Fig. 2. Each step on the surface is treated as a one-dimensional continuum object in order to compute the boundary condition for the adatom diffusion equation on the terrace.

incorporated into the crystal (the details of this process is neglected in the original BCF model), we thus have

$$\frac{1}{a^2} \mathbf{v} \cdot \mathbf{n} = J_+ + J_- \tag{7}$$

where a is the lattice constant of the crystal and hence $\frac{1}{a^2}$ denotes the atom density.

The system of equations (1), (4), (5) and (7) (or (1), (6) and (7)) completely determines the evolution of the steps.

2.2. Generalized BCF Theory

The generalization of the BCF theory considered here takes into account in more detail the incorporation process at the steps. In order to do this, we examine the dynamics of the *edge adatoms*. These are the adatoms residing on the edge (step). They differ from the terrace adatoms by having at least one more neighboring atom. Hence the edge adatoms are much less mobile than the terrace adatoms. One can also think of the steps as being a one-dimensional potential well along which the edge adatoms diffuse.

Denote by φ the edge adatom number density (with unit length^{-1}). The constitutive relations for J_+ and J_- are now changed to

$$J_+ = -\left(D \frac{\partial \rho}{\partial n} + \rho \mathbf{v} \cdot \mathbf{n} \right)\Big|_+ = \alpha_+ \rho - \beta_+ \varphi \tag{8}$$

$$J_- = \left(D \frac{\partial \rho}{\partial n} + \rho \mathbf{v} \cdot \mathbf{n} \right)\Big|_- = \alpha_- \rho - \beta_- \varphi \tag{9}$$

where β_+ and β_- are the hopping rates of edge adatoms *back* to the lower and upper terraces.

The dynamical equation for φ is specified by the conservation of adatoms

$$\frac{D\varphi}{Dt} = J_+ + J_- - \frac{1}{a^2} v \tag{10}$$

where $\frac{D}{Dt}$ refers to the *material derivative* as the steps are actually moving. (Its precise form will be given when we write down the continuum limit (35).)

A constitutive relation has to be given to v. Again it is natural to postulate a linear relation:

$$v = a^2 k(\gamma\varphi - \delta) \tag{11}$$

where k is the kink density. At each kink site, $\gamma\varphi$ is the flux of edge adatoms into the kinks and δ is the flux of attached adatoms out of the kinks. (Such a form for the step velocity has also been used in ref. 4, Sections II.13 and III.4).

Compared with the BCF model described in Section 2.1, the present model ((1), (8)–(11)) takes into account the dynamics of both the terrace and edge adatoms. For this reason, we call this the **TE-Model** and the original BCF theory the **T-Model**. In this spirit, the system of equations in ref. 4 which considers furthermore the dynamics of kinks should be called the **TEK-Model**.

2.3. Relation Between the T and TE-Models

In this section, we show that the **T-Model** can in fact be recovered from the **TE-Model** if the dynamics of φ reaches its *kinetic equilibrium*. This seems to show that the essential difference between the models lies on the *relative rates* of the different processes.

By setting $\frac{d\varphi_j}{dt} = J_j^+ + J_j^- - \frac{v_j}{a^2} = 0$, i.e., $\alpha_+\rho_j^+ + \alpha_-\rho_j^- - (\beta_+ + \beta_-)\,\varphi_j = k\gamma\varphi_j - k\delta$, we obtain the following equilibrium value for φ_j:

$$\varphi_j = \frac{\alpha_+\rho_j^+ + \alpha_-\rho_j^- + k\delta}{\beta_+ + \beta_- + k\gamma} \tag{12}$$

Now the fluxes in the **TE-Model** become:

$$\begin{aligned} J_j^+ &= \alpha_+\rho_j^+ - \beta_+\left(\frac{\alpha_+\rho_j^+ + \alpha_-\rho_j^- + k\delta}{\beta_+ + \beta_- + k\gamma}\right) \\ &= \left(\frac{\beta_- + k\gamma}{\beta_+ + \beta_- + k\gamma}\right)\alpha_+\rho_j^+ - \left(\frac{\beta_+}{\beta_+ + \beta_- + k\gamma}\right)\alpha_-\rho_j^- - \left(\frac{\beta_+ k\delta}{\beta_+ + \beta_- + k\gamma}\right) \end{aligned} \tag{13}$$

$$\begin{aligned} J_j^- &= \alpha_-\rho_j^- - \beta_-\left(\frac{\alpha_+\rho_j^+ + \alpha_-\rho_j^- + k\delta}{\beta_+ + \beta_- + k\gamma}\right) \\ &= \left(\frac{\beta_+ + k\gamma}{\beta_+ + \beta_- + k\gamma}\right)\alpha_-\rho_j^- - \left(\frac{\beta_-}{\beta_+ + \beta_- + k\gamma}\right)\alpha_+\rho_j^+ - \left(\frac{\beta_- k\delta}{\beta_+ + \beta_- + k\gamma}\right) \end{aligned} \tag{14}$$

If we consider the following regime for the parameters:

$$\beta_\pm \ll k\gamma, \qquad \rho_j^\pm \sim \frac{\beta_\pm \delta}{\alpha_\pm \gamma} \tag{15}$$

then the fluxes are further simplified to

$$J_j^+ = \alpha_+ (\rho_j^+ - \rho_e^+) \qquad \text{where} \quad \rho_e^+ = \frac{\beta_+ \delta}{\alpha_+ \gamma} \tag{16}$$

$$J_j^- = \alpha_- (\rho_j^- - \rho_e^-) \qquad \text{where} \quad \rho_e^- = \frac{\beta_- \delta}{\alpha_- \gamma} \tag{17}$$

so that (a variant of) the **T-Model** is recovered.

The scaling in (15) means that the dynamical processes between the edge adatoms and the kinks are much faster than the detachment of the edge adatoms back to the terraces. The quantities $\rho_e^\pm$ can be regarded as the *equilibrium* terrace adatom densities. By imposing $\alpha_+ \beta_- = \alpha_- \beta_+$ or $\beta_\pm \delta \ll \alpha_\pm \gamma$, we arrive at $\rho_e^+ = \rho_e^-$ or $\rho_e^+ = \rho_e^- = 0$.

Similar type of reasoning can also be carried out to link the **TEK-Model** introduced in ref. 4 to our **TE-Model**.

2.4. Other Models

In this section, we mention some other physical models that are often used to describe epitaxial growth.

Adatom Permeability or Leakage Model. One of the main features of our **TE-Model** (and also the **TEK-Model** in ref. 4) is that it allows the possibility of *longer range diffusion* for the terrace adatoms as they can hop across the step to upper or lower terraces. There are some other approaches which can also achieve similar effects. All of these models allow certain *leakage* or *permeability* of the terrace adatoms from one terrace to another (see refs. 5 and 24). Mathematically, the fluxes are formulated as:

$$J_j^+ = \alpha_+ \rho_j^+ - \beta_+ \rho_j^-$$
$$J_j^- = \alpha_- \rho_j^- - \beta_- \rho_j^+.$$

We anticipate that they will lead to a similar type of system to our **TE-Model**.

Step Interaction Models. The interactions between the steps can come from either *entropic* or *elastic* considerations. To incorporate these effects, the fluxes are modeled as:

$$J_j^+ = \alpha_+(\rho_j^+ - \mu_j)$$
$$J_j^- = \alpha_-(\rho_j^- - \mu_j).$$

Here μ_j is the *chemical potential* of a step which in general depends on the neighboring step configurations. For example, in refs. 9 and 16, μ_j is taken to be:

$$\mu_j = K\left(\frac{1}{l_j^3} - \frac{1}{l_{j-1}^3}\right).$$

It would also be interesting to consider the continuum limits of these types of models.

With the above introduction, we now proceed to derive the continuum limits for the **T-** and **TE-Models**. We will first concentrate on the $1+1$ dimensions. Higher dimensional formulations will be mentioned at the end.

3. CONTINUUM LIMITS OF VICINAL SURFACE (1 + 1 DIMENSION)

Vicinal terraces are those that are bounded by one up- and one down-step (Fig. 3). *Top(bottom)* terraces are bounded by two down-steps(up-steps) and are the local maxima(minima) of the step profile. In the present work, we are interested in length scales larger than the typical terrace width but smaller than the typical distance between the peaks and valleys on the surface. In taking the continuum limit, the step profiles are replaced by a *continuous height function* $h(x, t)$.

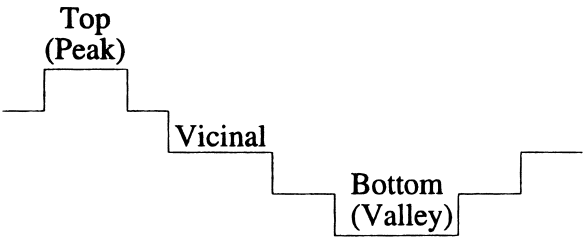

Fig. 3. In the one-dimensional setting, a typical surface structure consists of top, vicinal and bottom terraces.

We first consider vicinal surfaces where $h(x,t)$ is monotonically decreasing or increasing. The consideration of peaks and valleys at the continuum level will be given in the next section.

3.1. T-Model Without Evaporation

Consider a sequence of vicinal steps located at $\{x_j(t)\}_{j=-\infty}^{\infty}$ at time t such that the step profile is monotonically decreasing (Fig. 4). We want to find a function $h(x,t)$ so that $h(x_j(t),t)-h(x_{j+1}(t),t)\approx a$, where a is a small parameter denoting the lattice size or step height. We assume that the horizontal scale is such that the typical terrace width $l=x_{j+1}-x_j$ is of order a. Our goal is to obtain an equation (**continuum limit**) for h as $a\to 0$.

The *Peclet number* $Pe=\frac{va}{D}$, defined as the ratio between the step velocity and the hopping velocity of the terrace adatom is typically very small. This suggests that we can make the quasi-static approximation in which the adatom density on the terrace adjusts instantaneously to the step motions. In addition, we can also neglect the Stefan term $\mathbf{v}\cdot\mathbf{n}$ in the boundary conditions (4) and (5). If we further assume that $\rho_e=0$, then the BCF equations (1), (4), (5) and (7) (without evaporation) simply become

$$\begin{array}{c}\textbf{Simplified BCF}\\ \textbf{(T}-\textbf{Model)}\end{array}\begin{cases} D\rho_{xx}=-F, & x\in(x_j(t),x_{j+1}(t))\\ D\rho_x|_j^+=\alpha_+\rho_j^+, \qquad -D\rho_x|_j^-=\alpha_-\rho_j^- & x=x_j(t)^{\pm}\\ v_j=\alpha_+\rho_j^++\alpha_-\rho_j^-=[D\rho_x]_j=D\rho_x|_j^+-D\rho_x|_j^- \end{cases}\qquad \text{(1}$$

The above system of equations can be solved explicitly. Let $l_j(t)=x_{j+1}(t)-x_j(t)$ be the terrace width. Then

$$\rho_j^+=\frac{Fl_j(D+\frac{1}{2}\alpha_-l_j)}{(\alpha_++\alpha_-)D+\alpha_+\alpha_-l_j},\qquad \rho_j^-=\frac{Fl_{j-1}(D+\frac{1}{2}\alpha_+l_{j-1})}{(\alpha_++\alpha_-)D+\alpha_+\alpha_-l_{j-1}}\qquad (19)$$

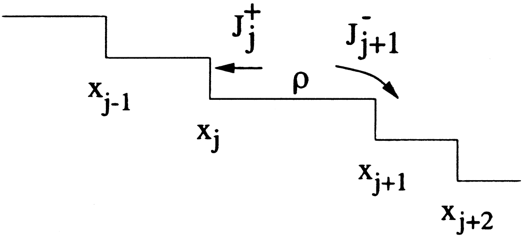

Fig. 4. ρ denotes the adatom density on a terrace. J_j^+ and J_j^- refers to the fluxes of terrace adatoms to the upper and lower steps. The x_j's refers to the (horizontal) locations of the steps.

Observe that

$$\alpha_+ \rho_j^+ + \alpha_- \rho_{j+1}^- = F l_j. \tag{20}$$

Using (19), the velocity of each step is given by

$$\frac{1}{a^2} v_j = \alpha_+ \rho_j^+ + \alpha_- \rho_j^- = \frac{F l_j (\alpha_+ D + \frac{1}{2}\alpha_+ \alpha_- l_j)}{(\alpha_+ + \alpha_-) D + \alpha_+ \alpha_- l_j} + \frac{F l_{j-1} (\alpha_- D + \frac{1}{2}\alpha_+ \alpha_- l_{j-1})}{(\alpha_+ + \alpha_-) D + \alpha_+ \alpha_- l_{j-1}} \tag{21}$$

To obtain the continuum limit, we let $a \to 0$ and set $D = O(a)\,\alpha_\pm$. In this way, we have $\frac{a}{l_j} \approx |h_x|\,(x_j, t)$ and $v_j = \frac{Fa^3}{|h_x|\,(x_j, t)}$. Since $v = \frac{h_t}{|h_x|}$, we arrive at the following

Continuum limit of T-Model for vicinal surface:

$$h_t = F a^3. \tag{22}$$

The above equation states that the height of the film increases *uniformly* across the interface. This is not surprising since the the **T-Model** simply describes the process that adatoms flow *irreversibly* to the nearest step. Therefore (22) is the obvious consequence of (20) which states that adatoms on the terraces are incorporated either at the nearest upper or lower steps. In particular, there is no possibility for the adatoms to diffuse across a step. In this case, it is natural to consider the next order effects as is done in the literature. This will be illustrated in the next section.

3.2. Modified Equation for T-Model

Here we consider a more general velocity law than (21):

$$\frac{1}{a^2} v_j = f(l_j) + g(l_{j-1}) \tag{23}$$

where f and g are the fluxes of adatoms from the lower and upper terraces to the jth step. Usually f and g are increasing functions of the terrace length l. By considering the following *second order* Taylor expansion for l, we have:

$$l_j = \frac{a}{|h_x|} + \frac{a^2 h_{xx}}{2|h_x|^3}, \qquad l_{j-1} = \frac{a}{|h_x|} - \frac{a^2 h_{xx}}{2|h_x|^3}.$$

Then the modified equation for h is given by:

$$\begin{aligned} h_t = v\,|h_x| &= \left(f\left(\frac{a}{|h_x|}+\frac{a^2 h_{xx}}{2|h_x|^3}\right)+g\left(\frac{a}{|h_x|}-\frac{a^2 h_{xx}}{2|h_x|^3}\right)\right) a^2\,|h_x| \\ &= \left(f\left(\frac{a}{|h_x|}\right)+g\left(\frac{a}{|h_x|}\right)\right) a^2\,|h_x| + \left(f'\left(\frac{a}{|h_x|}\right)-g'\left(\frac{a}{|h_x|}\right)\right)\frac{a^4 h_{xx}}{2\,|h_x|^2} \end{aligned} \tag{24}$$

If we substitute formula (21) for f and g, the above equation becomes

$$h_t = Fa^3 + \left(\frac{F(\alpha_+ - \alpha_-)\,\bar{\alpha} D^2}{2(\bar{\alpha} D\,|h_x| + \pi a)^2}\right) a^4 h_{xx}. \tag{25}$$

By introducing the quantity $\tilde{h} = h - Fa^3 t$ which describes the evolution of the film in a *moving frame*, we arrive at the following equation:

$$\tilde{h}_t = \left(\frac{F(\alpha_+ - \alpha_-)\,\bar{\alpha} D^2}{2(\bar{\alpha} D\,|\tilde{h}_x| + \pi a)^2}\right) a^4 \tilde{h}_{xx}. \tag{26}$$

Similar computations have also been done in ref. 11.

Note that Eq. (26) is a forward heat equation if $\alpha_+ > \alpha_-$. It reflects the fact that the one dimensional **T-Model** in the step flow regime is a *stable* evolution.

3.3. TE-Model Without Evaporation

As in the **T-Model**, we still work in the regime when $Pe \ll 1$. Then (1), (8)–(11) (without evaporation) is simplified to

$$\begin{array}{c} \textbf{Generalized BCF} \\ \textbf{(TE} - \textbf{Model)} \end{array} \left\{ \begin{aligned} D\rho_{xx} &= -F \\ D\rho_x|_j^+ &= \alpha_+ \rho_j^+ - \beta_+ \varphi_j = J_j^+ \\ -D\rho_x|_j^- &= \alpha_- \rho_j^- - \beta_- \varphi_j = J_j^- \\ \frac{d\varphi_j}{dt} &= \dot{\varphi}_j = J_j^+ + J_j^- - \frac{v_j}{a^2} \\ v_j &= a^2 k(\gamma\varphi_j - \delta) \end{aligned} \right. \tag{27}$$

In this case, ρ can be solved in terms of φ which act as boundary values for the diffusion equation (1). The solution is given by:

$$\rho_j^+ = \frac{Fl_j(D+\frac{1}{2}\alpha_- l_j)}{\bar{\alpha}D+\pi l_j} + \left(\frac{(D+\alpha_- l_j)\beta_+}{\bar{\alpha}D+\pi l_j}\right)\varphi_j + \left(\frac{D\beta_-}{\bar{\alpha}D+\pi l_j}\right)\varphi_{j+1} \tag{28}$$

$$\rho_j^- = \frac{Fl_{j-1}(D+\frac{1}{2}\alpha_+ l_{j-1})}{\bar{\alpha}D+\pi l_{j-1}} + \left(\frac{D\beta_+}{\bar{\alpha}D+\pi l_{j-1}}\right)\varphi_{j-1} + \left(\frac{(D+\alpha_+ l_{j-1})\beta_-}{\bar{\alpha}D+\pi l_{j-1}}\right)\varphi_j \tag{29}$$

$$J_j^+ = \frac{\alpha_+ Fl_j(D+\frac{1}{2}\alpha_- l_j)}{\bar{\alpha}D+\pi l_j} + \left(\frac{DQ}{\bar{\alpha}D+\pi l_j}\right)\varphi_j + \left(\frac{D\alpha_+\beta_-}{\bar{\alpha}D+\pi l_j}\right)(\varphi_{j+1}-\varphi_j) \tag{30}$$

$$J_j^- = \frac{\alpha_- Fl_{j-1}(D+\frac{1}{2}\alpha_+ l_{j-1})}{\bar{\alpha}D+\pi l_{j-1}} - \left(\frac{DQ}{\bar{\alpha}D+\pi l_{j-1}}\right)\varphi_{j-1} - \left(\frac{D\alpha_+\beta_-}{\bar{\alpha}D+\pi l_{j-1}}\right)(\varphi_j-\varphi_{j-1}) \tag{31}$$

where we have used the notation $\bar{\alpha}=\alpha_+ + \alpha_-$, $\pi = \alpha_+\alpha_-$ and $Q=\alpha_+\beta_- - \alpha_-\beta_+$. Hence

$$\begin{aligned}
\frac{d\varphi_j}{dt} &= \dot{\varphi}_j = J_j^+ + J_j^- - \frac{v}{a^2} \\
&= \frac{\alpha_+ Fl_j(D+\frac{1}{2}\alpha_- l_j)}{\bar{\alpha}D+\pi l_j} + \frac{\alpha_- Fl_{j-1}(D+\frac{1}{2}\alpha_+ l_{j-1})}{\bar{\alpha}D+\pi l_{j-1}} \\
&\quad + D\left(\frac{\alpha_+\beta_- + \alpha_-\beta_+}{2}\right)\left(\frac{\varphi_{j+1}-\varphi_j}{\bar{\alpha}D+\pi l_j} - \frac{\varphi_j-\varphi_{j-1}}{\bar{\alpha}D+\pi l_{j-1}}\right) \\
&\quad + D\left(\frac{\alpha_+\beta_- - \alpha_-\beta_+}{2}\right)\left(\frac{\varphi_{j+1}+\varphi_j}{\bar{\alpha}D+\pi l_j} - \frac{\varphi_j+\varphi_{j-1}}{\bar{\alpha}D+\pi l_{j-1}}\right) \\
&\quad - \frac{v}{a^2}
\end{aligned} \tag{32}$$

The above formulas are exact given the approximations made in (27). It is then quite easy to extract from (32) the following *leading order* continuum equations for φ and h.

Continuum limit of TE-Model for vicinal surface:

$$\frac{D\varphi}{Dt} = \frac{aF}{|h_x|} + a\partial_h(A(|h_x|)\,\partial_h\varphi) \pm 2\left(\frac{\alpha_+\beta_- - \alpha_-\beta_+}{\alpha_+\beta_- + \alpha_-\beta_-}\right)\partial_h(A(|h_x|)\,\varphi) - \frac{v}{a^2} \tag{33}$$

$$v = a^2k(\gamma\varphi-\delta), \qquad h_t = v\,|h_x| = a^2k(\gamma\varphi-\delta)\,|h_x| \tag{34}$$

where

$$\frac{D\varphi}{Dt} = \frac{d\varphi(x(t),t)}{dt} = \frac{\partial\varphi}{\partial t} \pm v\frac{\partial\varphi}{\partial x} \tag{35}$$

$$A(|h_x|) = \left(\frac{\alpha_+\beta_- + \alpha_-\beta_+}{2}\right)\frac{aD\,|h_x|}{(\alpha_+ + \alpha_-)\,D\,|h_x| + \alpha_+\alpha_-a} \tag{36}$$

$$\partial_h = \frac{1}{|h_x|}\,\partial_x, \qquad \pm = -\operatorname{sgn}(h_x) \tag{37}$$

The sign convention for v is that it points to the lower terrace.

In writing down the above equations, we have considered the following scaling for the parameters:

$$a = \text{ lattice height} \to 0 \tag{38}$$

$$l = O(a) = \frac{a}{|h_x|} \tag{39}$$

$$\varphi = O(1) \tag{40}$$

$$h,\, h_x = O(1) \tag{41}$$

$$\alpha_+,\, \alpha_- = \alpha = O(1) \tag{42}$$

$$\beta_+,\, \beta_- = \beta = O(1) \tag{43}$$

$$D = O(a)\,\alpha \tag{44}$$

$$F = O(a)\,\beta\varphi \tag{45}$$

$$Q = \alpha_+\beta_- - \alpha_-\beta_+ = O(a)\,\alpha\beta \tag{46}$$

The above lead to the following:

$$(\alpha_+ + \alpha_-)\,D + \alpha_+\alpha_- = O(a)\,\alpha^2$$

$$A(|h_x|) = O(a)\,\beta$$

$$\frac{D\varphi}{Dt} = O(a^2\beta)\,\varphi.$$

Even though not all terms in (33) are of the same order, we keep the leading order behavior of each of the following effects: *deposition, diffusion, convection* and *incorporations*.

Equations (33) and (34) constitute the coupled system we announced at the beginning. They show the fact that edge adatoms are able to diffuse *across the terraces*. This diffusion is hence much more global than just the terrace diffusion considered in the original BCF theory. This is described by the second term of the right hand side of (33). The third term is a drift due to the *Schwoebel barrier* (to be explained below). The fourth term is the loss to the growing interface.

It is instructive to rewrite (33) as

$$\frac{|h_x|}{a}\frac{D\varphi}{Dt}+\frac{1}{a^3}\frac{\partial h}{\partial t}=F+\partial_x(\varphi\tilde{A}(h_x)\,\partial_x\mu) \tag{47}$$

where

$$\mu=kT\left(\ln\varphi+2\,\mathrm{sgn}(h_x)\left(\frac{\alpha_+\beta_- -\alpha_-\beta_+}{\alpha_+\beta_- +\alpha_-\beta_+}\right)\frac{h}{a}\right), \tag{48}$$

$$\tilde{A}(h_x)=\frac{1}{kT}\frac{A(h_x)}{|h_x|}=\frac{1}{2kT}\frac{a(\alpha_+\beta_- +\alpha_-\beta_+)\,D}{(\alpha_+ +\alpha_-)\,D\,|h_x|+\alpha_+\alpha_-a}. \tag{49}$$

Here k and T are respectively the Boltzmann constant and temperature. Clearly μ should be interpreted as the *chemical potential*. The first term in μ is the usual entropic factor. The second term resembles the standard gravitational potential. It is caused by the Schwoebel barrier. In general, such barrier refers to the asymmetry of the hopping processes between upper and lower terraces at the step edges, i.e., either $\alpha_+\neq\alpha_-$ or $\beta_+\neq\beta_-$ or both. Usually, $\alpha_+>\alpha_-$ and $\beta_+>\beta_-$. Physically, it represents an additional step-edge barrier that have to be overcome by the adatoms to diffuse across the step edges. In the present setting, the effect of this step-edge barrier is described by the coefficient $\frac{\alpha_+\beta_- -\alpha_-\beta_+}{\alpha_+\beta_- +\alpha_-\beta_+}$. The number $\tilde{A}(h_x)$ represents the *effective diffusion coefficient*. Its form shows that the presense of steps slows down diffusion. (Note that $\tilde{A}(h_x)\to 0$ as $|h_x|\to\infty$.) This slowing down is not caused by the Schwoebel barrier but rather by the inhomogeneous environment created by the steps.

Remark 1. In the present formulation of the continuum limit (33) and (34), we use φ and h as the unknown variables. The terrace adatom density ρ is eliminated. However, we can also use ρ and h as the variables. To do this, we define $\bar{\rho}_j=\frac{1}{2}(\rho_j^+ +\rho_{j+1}^-)$. Then at the continuum level, $\bar{\rho}$ and φ are proportional to each other:

$$\bar{\rho}=\frac{2\beta_+\beta_-}{\alpha_+\beta_- +\alpha_-\beta_+}\varphi. \tag{50}$$

Hence, φ can be eliminated and the continuum equations become

$$\frac{D\bar{\rho}}{Dt}=\frac{2\beta_+\beta_-}{\alpha_+\beta_-+\alpha_-\beta_+}\frac{aF}{|h_x|}+a\partial_h(A(|h_x|)\,\partial_h\bar{\rho})\pm 2\left(\frac{\alpha_+\beta_--\alpha_-\beta_+}{\alpha_+\beta_-+\alpha_-\beta_-}\right)\partial_h(A(|h_x|)\,\bar{\rho})$$
$$-\frac{2\beta_+\beta_-}{\alpha_+\beta_-+\alpha_-\beta_+}\frac{v}{a^2}\tag{51}$$

$$v=a^2k\left(\gamma\frac{\alpha_+\beta_-+\alpha_-\beta_+}{2\beta_+\beta_-}\bar{\rho}-\delta\right)\quad\blacksquare\tag{52}$$

Remark 2. The relationship between the **T-** and **TE-Models** can also be established at the continuum level in a similar way as in Section 2.3. By (33), the kinetic equilibrium condition for φ implies:

$$k(\gamma\varphi-\delta)-a\partial_h(A(|h_x|)\,\partial_h\varphi)-2\left(\frac{\alpha_+\beta_--\alpha_-\beta_+}{\alpha_+\beta_-+\alpha_-\beta_-}\right)\partial_h(A(|h_x|)\,\varphi)=\frac{aF}{|h_x|}$$

Thus φ solves an *elliptic* problem which in term determines the step velocity by (11). Under the same scaling regime for $\beta_\pm$ as in (15), it can be shown that the second and third terms of the left hand side are much smaller than the first term as $a\to 0$. So we still have

$$v=a^2k(\gamma\varphi-\delta)=\frac{a^3F}{|h_x|}$$

which is the same as the **T-Model**. ∎

4. BOUNDARY CONDITIONS AT VALLEYS AND PEAKS

Our discussion so far is restricted to vicinal surfaces. The equations apply to growth via step flows. We next consider the conditions at mountain peaks and valleys which are generally present in island growth (Fig. 5). Our approach is to supplement the continuum equations by appropriate boundary conditions at these points. As the locations of the mountain peaks and valleys might be time dependent, the whole evolution then becomes a free boundary problem. While a complete set of conditions at the valleys can be obtained through geometric and conservation considerations, conditions at the peaks are associated with an entirely new physical process, namely nucleation. We anticipate that additional constitutive relations have to be imposed at the peaks in order to fully describe the nucleation phenomena. One can draw an analogy between the valleys/peaks and

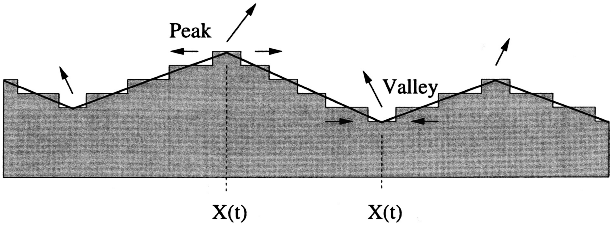

Fig. 5. A continuum description of a typical surface structure treats the peaks and valleys as free boundary points located at $x(t)$'s.

shocks/rarefaction waves in hydrodynamics. Only that in the present case, the relevant flux is $f(u) = |u|$ so that the rarefaction waves can also be discontinuous.

4.1. Continuum Limit in Eulerian Coordinates

In order to write down the boundary conditions, it is convenient to reformulate the continuum equation (33) in terms of the Eulerian coordinates. We first define the edge adatom density *per unit length* as $\Phi = |h_x| \varphi$. Then (33) becomes

$$\frac{\partial \Phi}{\partial t} - (\Phi v)_x = aF + \partial_x(\mathcal{J}_+) - \frac{1}{a^2} h_t, \qquad \text{for} \quad h_x > 0 \tag{53}$$

$$\frac{\partial \Phi}{\partial t} + (\Phi v)_x = aF + \partial_x(\mathcal{J}_-) - \frac{1}{a^2} h_t, \qquad \text{for} \quad h_x < 0 \tag{54}$$

where

$$\mathcal{J}_+ = a\tilde{A}(h_x)\, \partial_x \frac{\Phi}{|h_x|} - 2\left(\frac{\alpha_+ \beta_- - \alpha_- \beta_+}{\alpha_+ \beta_- + \alpha_- \beta_+}\right) \tilde{A}(h_x)\, \Phi \tag{55}$$

$$\mathcal{J}_- = a\tilde{A}(h_x)\, \partial_x \frac{\Phi}{|h_x|} + 2\left(\frac{\alpha_+ \beta_- - \alpha_- \beta_+}{\alpha_+ \beta_- + \alpha_- \beta_+}\right) \tilde{A}(h_x)\, \Phi \tag{56}$$

(Recall the sign convention that v is pointing to the lower terrace.)

In the following, we will use $X(t)$ to denote the location of the valleys or peaks. At each valley, we have[3] $h_x(X(t)^-) < 0$ and $h_x(X(t)^+) > 0$ while at the peak $h_x(X(t)^-) > 0$ and $h_x(X(t)^+) < 0$ (Figure 5).

---

[3] We use the convention that subscript ± refers the regions with positive or negative slope while superscript ± refers to right or left limit of a function.

4.2. Boundary Conditions at Valleys

As mentioned before, valleys are like shocks–the characteristic curves intersect. This means that the steps are coming together from both sides of the valley and are annihilated.

In the present setting, we have the usual Rankine–Hugoniot condition corresponding to the *conservation of adatoms*:

$$[\Phi]\dot{X}(t) = -(\mathscr{J}_+(X^+(t)) - \mathscr{J}_-(X^-(t))) - (\Phi v)(X(t)^+) - (\Phi v)(X(t)^-) \tag{57}$$

Since the height function is continuous, we obtain the following *geometric condition* by differentiating the relationship $h(X^+(t), t) = h(X^-(t), t)$ in time and using the fact that $h_t(X^\pm) = v\,|h_x|\,(X^\pm)$:

$$\dot{X}(t) = -\frac{|h_x v(X^+)| - |h_x v(X^-)|}{|h_x(X^+)| + |h_x(X^-)|} \tag{58}$$

In essence, this is the Rankine–Hugoniot condition for the equation $(h_x)_t = (v\,|h_x|)_x$.

In addition, because of the presence of diffusion flux in (53) and (54), it is natural to impose the *continuity of the chemical potential* $[\mu] = 0$ at the valley. This leads to

$$[\varphi] = \left[\frac{\Phi}{|h_x|}\right] = 0 \tag{59}$$

This set of boundary conditions (57), (58) and (59) completely specifies the evolution of the film at the valley.

4.3. Boundary Conditions at Peaks

As the peaks evolve like rarefaction waves—the steps on both sides are moving away from each other, we anticipate the need for extra boundary condition(s) to determine the growth of h in the space between the separating steps. The conservation and geometric conditions (57) and (58) for the valley are still valid at the peak (with some sign changes):

$$[\Phi]\dot{X}(t) = -(\mathscr{J}_+(X^+(t)) - \mathscr{J}_-(X^-(t))) + (\Phi v)(X(t)^+) + (\Phi v)(X(t)^-) \tag{60}$$

$$\dot{X}(t) = \frac{|h_x v(X^+)| - |h_x v(X^-)|}{|h_x(X^+)| + |h_x(X^-)|} \tag{61}$$

However, we do not expect the continuity of φ to be valid at the peak due to the possibility of nucleations. So we are lacking *two more* boundary conditions—one for the *horizontal velocity* $\dot{X}(t)$ and one for the *vertical velocity* V of the peak. At this level of the continuum limit, we can specify arbitrary values for these velocities. It is probable that we need to look into the nucleation process in order to relate the values of $\dot{X}(t)$ and V to more microscopic physical parameters.

Remark. The need for two more boundary conditions can also be understood in the following way.

Given h (or $h_x(X^+)$ and $h_x(X^-)$) at a certain time, $\dot{X}(t)$ needs to be prescribed to solve the Φ diffusion equations (53) and (54) with the two boundary conditions (60) and (61). This will then determine $\Phi(X^+)$ and $\Phi(X^-)$ and hence $v(X^+)$ and $v(X^-)$. The next step is to solve $h_t = v\,|h_x|$ with rarefaction wave initial data, for example $-|x|$. In order to have unique solution, we need further to specify the vertical growth rate V in addition to the horizontal peak velocity $\dot{X}(t)$. ▮

5. CONTINUUM LIMITS IN 2 + 1 DIMENSIONS

In this section, we describe the continuum limits in $2+1$ dimensions for the **TE-Model**. (The **T-Model** remains unchanged.) As before, we consider a family of vicinal steps. Now each step is a one dimensional curve which can be parametrized by its *arclength* s. The differences with the $1+1$ dimensional case are that now φ_j is a function of s and t and the edge adatoms can also diffuse along the edge with some diffusion constant D_e. So the dynamical equation (10) for φ_j is changed to

$$\frac{d\varphi_j}{dt} = D_e \partial_s^2 \varphi_j + J_j^+ + J_j^- - \frac{1}{a^2} v_j \tag{62}$$

In passing to the continuum limit, we must note the difference between the independent variables s and n. s is the coordinate *along* a step which is a *level set* of the height function h and n is the coordinate *normal* to the step. s is the *slow* variable which acts as a parameter whereas n is the *fast* variable over which homogenization takes place. With this in mind, we can easily write down the continuum equations in a form similar to (47):

$$\frac{|\nabla h|}{a}\left(\frac{D\varphi}{Dt} + \varphi \kappa v\right) + \frac{1}{a^3}\frac{\partial h}{\partial t} = F + \nabla \cdot (\varphi M(|\nabla h|)\,\nabla \mu) \tag{63}$$

where

$$\frac{D}{Dt}=\frac{\partial}{\partial t}+v\hat{n}\cdot\nabla;$$

$$\hat{n}=-\frac{\nabla h}{|\nabla h|}$$

$$\nabla=(\partial_s,\partial_n)=\left(\frac{\nabla^{\perp}h}{|\nabla h|}\cdot\nabla,\ -\frac{\nabla h}{|\nabla h|}\cdot\nabla\right)$$

$$\nabla=(\partial_x,\partial_y),\qquad \nabla^{\perp}=(-\partial_y,\partial_x),$$

$$M(|\nabla h|)=\begin{pmatrix} D_e & 0\\ 0 & \tilde{A}(|\nabla h|)\end{pmatrix}$$

$$\kappa=\nabla\cdot\hat{n}=\nabla\cdot\left(-\frac{\nabla h}{|\nabla h|}\right)=\text{curvature of the level set of } h.$$

and $\tilde{A}(|\nabla h|)$ is the same as (49). We still have

$$\partial_t h=v\,|\nabla h|,\qquad v=a^2k(\hat{n})(\gamma\varphi-\delta).\tag{64}$$

Remark 1. The derivation of (63) is done by considering the following conservation law:

$$\frac{d}{dt}\int_{\Gamma_j(t)\cap\mathcal{O}}\varphi_j(s,t)\,ds=\int_{\Gamma_j(t)\cap\mathcal{O}}\left(J_j^{+}+J_j^{-}-\frac{v}{a^2}\right)ds+D_e\partial_s\varphi(s_1,t)-D_e\partial_s\varphi(s_2,t)$$

where $\Gamma_j(t)$ is the jth step parametrized by arclength s and $\mathcal{O}$ is some open set intersecting $\Gamma_j(t)$ at just two points s_1 and s_2. The left hand side of the above equals

$$\int_{\Gamma_j(t)\cap\mathcal{O}}(\varphi_t+v\hat{n}\cdot\nabla\varphi+\varphi\kappa v)\,ds$$

which gives (63). ∎

Remark 2. It is again convenient to rewrite (63) in terms of the variable $\Phi=\varphi\,|\nabla h|$:

$$\Phi_t+\nabla\cdot(\Phi v\hat{n})=F+\nabla\cdot\left(\frac{\Phi}{|\nabla h|}M(|\nabla h|)\,\nabla\mu\right)-\frac{1}{a^2}h_t\tag{65}$$

where we have used the following identity

$$\nabla\cdot(\Phi v\hat{n})=\hat{n}\cdot\nabla(\Phi v)+\Phi v\nabla\cdot\hat{n}.\quad ∎$$

5.1. Boundary Conditions at the Valleys and Peaks

As in the $1+1$ dimensions, we need to impose appropriate boundary conditions at the valleys and peaks. We consider a general surface morphology such that the valleys are along *curves* and peaks are at *isolated points*.

The boundary conditions at the valleys are quite similar to the $1+1$ dimensional case. They include the conservation of adatoms, geometric condition and the continuity of the chemical potential μ across the valley. If we denote the location of the valley at time t by $X(\cdot, t)$, then these boundary conditions are expressed as follow:

$$\left([\Phi]\dot{X} + \left[\frac{\Phi}{|\nabla h|} M(|\nabla h|)\, \nabla \mu \right] - [\Phi v \hat{n}] \right) \cdot \hat{n} = 0 \tag{66}$$

$$[\nabla h] \cdot \dot{X} + [v\, |\nabla h|] = 0 \tag{67}$$

$$\left[\frac{\Phi}{|\nabla h|} \right] = 0 \tag{68}$$

where $[f] =$ the jump in the value of f across the valley.

At the peak, the situation is slightly different. As the singularities are isolated points, the diffusion equation (65) can be solved everywhere in the neighborhood of these points. No extra boundary conditions need to be specified. This situation is similar to solving the Laplace equation in a punctured disk: any L^∞ solution can be extended to a solution on the whole disk. Hence the velocities v of the steps (or equivalently the level sets of h) near the peak are completely determined by just solving (65) alone.

The next step is to solve $h_t = v\,|\nabla h|$ with rarefaction initial data such as $h(0, (x, y)) = -\sqrt{x^2+y^2}$. The geometric condition can be used to determine the *horizontal velocity* of the peak in the following way. Let $X(t)$ be the location of the peak and $\hat{n}_\theta$ be the horizontal unit vector which makes an angle θ with some reference coordinate axis. The notation $f(X_\theta^\pm)$ refers to the one-sided limiting value of f at $X(t)$ taken along $\pm\hat{n}_\theta$. By the continuity of the height profile, we have $h(X_\theta^-, t) = h(X_\theta^+, t)$. Differentiating in time gives

$$(\nabla h(X_\theta^-) \cdot \hat{n}_\theta)(\dot{X} \cdot \hat{n}_\theta) + h_t(X_\theta^-) = (\nabla h(X_\theta^+) \cdot \hat{n}_\theta)(\dot{X} \cdot \hat{n}_\theta) + h_t(X_\theta^+).$$

Using the fact that $h_t(X_\theta^\pm) = v(X_\theta^\pm)\, |\nabla h(X_\theta^\pm)|$, we arrive at the following identity which is true *for all* θ:

$$\dot{X} \cdot \hat{n}_\theta = \frac{v(X_\theta^+)\, |\nabla h(X_\theta^+)\,| - v(X_\theta^-)|\, \nabla h(X_\theta^-)|}{\nabla h(X_\theta^-) \cdot \hat{n}_\theta - \nabla h(X_\theta^+) \cdot \hat{n}_\theta} \tag{69}$$

This then uniquely prescribes $\dot{X}$. The *vertical velocity* still needs to be determined, probably from the underlying nucleation process.

6. TE-MODEL WITH VAPOR PHASE DIFFUSION

In CVD growth, the adatoms are delivered to the interface through diffusion in the reactor. In this section, we present the continuum limit incorporating such a mechanism.

We first consider a one dimensional model. In order to describe the interfacial profile, we will use z and x to denote the spatial variables in the vertical and horizontal directions. As in the previous sections, we first study the case of a sequence of vicinal terraces and steps located at $\{z=z_j\}_{j=-\infty}^{\infty}$ and $\{x=x_j\}_{j=-\infty}^{\infty}$ so that $z_j - z_{j+1} = a$ and the step profile is monotonically decreasing (Fig. 6). In the present setting, we need to specify the evolution of three types of mobile atoms— *vapor, terrace* and *edge* adatoms. We will use Γ to denote the number density of the adatoms in the vapor phase (with unit = length^{-3}).

The diffusion of vapor adatoms can be described by the following equation for Γ which holds in the region above the interface:

$$\frac{\partial \Gamma}{\partial t} = D_b \triangle \Gamma = D_b(\partial_x^2 \Gamma + \partial_z^2 \Gamma). \tag{70}$$

The boundary conditions are

$$\Gamma(x, +\infty, t) = F, \qquad -\infty < x < \infty \tag{71}$$

$$D_b \frac{\partial \Gamma}{\partial z}(x, z_j, t) = \sigma \Gamma(x, z_j, t), \qquad x_j < x < x_{j+1} \tag{72}$$

$$D_b \frac{\partial \Gamma}{\partial x}(x_j, z, t) = \lambda \Gamma(x_j, z, t), \qquad z_j < z < z_{j+1}. \tag{73}$$

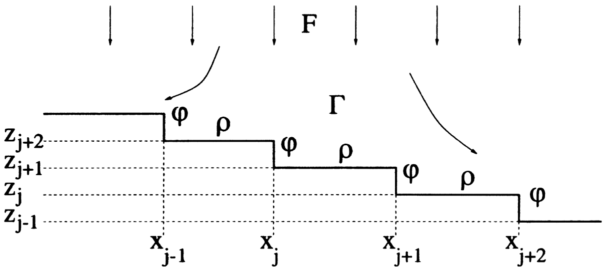

Fig. 6. In models incorporating vapor phase diffusion, we consider the densities of the mobile adatoms in the vapor phase (Γ), on the terrace (ρ) and at the step (φ). The x and z refer to the horizontal and vertical spatial variables.

Here F is some uniform deposition flux at infinity; σ and λ are the attachment rates of the vapor adatoms to the terraces and steps.

The terrace adatom density ρ solves an equation similar to (27):

$$0 = D\partial_x^2\rho + D_b\,\frac{\partial\Gamma}{\partial z}, \qquad z = z_j, \quad x_j < x < x_{j+1} \tag{74}$$

$$D\rho_x|_j^+ = \alpha_+\rho_j^+ - \beta_+\varphi_j = J_j^+, \qquad x = x_j^+ \tag{75}$$

$$-D\rho_x|_j^- = \alpha_-\rho_j^- - \beta_-\varphi_j = J_j^-, \qquad x = x_j^- \tag{76}$$

The rate of change of the edge adatom density φ is given by

$$\frac{d\varphi_j}{dt} = J_j^+ + J_j^- + D_b\int_{z_j}^{z_{j+1}} \frac{\partial\Gamma}{\partial x}(x_j, z, t)\,dz - \frac{v_j}{a^2}. \tag{77}$$

Note that we have allowed the possibility of the direct attachment of the vapor adatoms to the edges. This process can be turned off by setting $\lambda = 0$ in (73).

Finally, we impose the same condition (11) for the step velocity:

$$v_j = a^2(\gamma\varphi_j - \delta). \tag{11}$$

The system of Eqs. (70)–(77) and (11) completely determines the dynamics of the variables Γ, ρ, φ_j and v_j. The continuum limit in this case is a coupled system involving the diffusions of Γ and φ and the growth of the interfacial height h.

6.1. Continuum Limit of TE-Model with Vapor Diffusion

The solutions for (74)–(77) are very similar to those of (28)–(32). We can perform the same limiting process as in the **TE-Model** and arrive at the following continuum limit:[4]

$$\frac{\partial\Gamma}{\partial t} = D_\Gamma\triangle\Gamma = D_\Gamma(\partial_x^2\Gamma + \partial_z^2\Gamma) \qquad \text{for} \quad z > h(x,t), \tag{78}$$

$$D_b\,\frac{\partial\Gamma}{\partial n} = -(\sigma\cos\theta + \lambda\sin\theta)\Gamma, \qquad \text{at} \quad z = h(x,t) \tag{79}$$

$$\Gamma(x, +\infty, t) = F, \tag{80}$$

---

[4] We follow the same notation as in (33)–(37).

$$\frac{D\varphi}{Dt} = aD_b\Gamma(x, h(x,t))\left(\lambda + \frac{\sigma}{|h_x|}\right) + a\partial_h(A(|h_x|)\,\partial_h\varphi) + \left(\frac{\alpha_+\beta_- - \alpha_-\beta_+}{\alpha_+\beta_- + \alpha_-\beta_-}\right)\partial_h(A(|h_x|)\,\varphi) - \frac{v}{a^2} \tag{81}$$

$$v = a^2k(\gamma\varphi - \delta), \qquad h_t = v\,|h_x| = a^2k(\gamma\varphi - \delta)\,|h_x| \tag{82}$$

Here

$$n = \frac{(h_x, -1)}{\sqrt{1+h_x^2}} = \text{unit normal vector of the interface} \tag{83}$$

$$\tan\theta = |h_x|. \tag{84}$$

Remark. The condition (79) is the *effective* boundary condition at the continuum level. It is derived by taking the average of the *oscillatory* boundary conditions (72) and (73). Such an averaging process is carried out carefully in refs. 8 and 3. We will sketch it in **A.3**. ▮

7. CONCLUSION

In this paper, we have studied the continuum limit of step flow models. Our limiting equations take the form of a coupled system of convection-diffusion equation for the adatom density and a Hamilton–Jacobi equation for the film height function. Novel free boundary conditions are imposed at the peaks and valleys on the surface.

It is instructive to compare our results with the ones in the existing literature. In refs. 1 and 20, the large scale meandering of the steps was studied using long-wave expansion techniques. This pertains to the dynamics of unstable perturbations in the weakly nonlinear regime. In principle, the equations derived here should also be able to model this regime. In ref. 19, higher order equations are used to describe the profile of the film between peaks and valleys. Phenomenological equations of the type introduced in ref. 13 (see also ref. 27) concern with the spatial length scales much larger than the typical mound size which is the scale considered here.

Further validations are needed to assess this approach, particularly on the strategies to incorporate nucleation. This is the topic for a subsequent paper. In the step flow regime, a parallel study has been carried out from a more microscopic starting point (kinetic monte-carlo instead of BCF)(21) Extension to include elastic effects is considered in ref. 28.

A. APPENDIX

Here we include some derivations of the formulas and extensions of the models we have considered.

A.1. Derivation of (28)–(31)

The formulas (28) and (29) are derived by solving for ρ in terms of φ_0 and φ_1 in the following *cell problem*:

$$D\rho_{xx} = -F(x), \qquad x \in [0, l] \tag{85}$$

$$J_0^+ = D\rho_x(0) = \alpha_+ \rho(0) - \beta_+ \varphi_0 \tag{86}$$

$$J_1^- = -D\rho_x(l) = \alpha_- \rho(l) - \beta_+ \varphi_1 \tag{87}$$

Here we consider a general $F(x)$ rather than a constant deposition flux F.

From (85), we have

$$\rho_x(x) = \rho_x(0) - \frac{1}{D}\int_0^x F(s)\, ds$$

$$\rho(x) = \rho(0) + \rho_x(0)\, x - \frac{1}{D}\int_0^x \int_0^r F(s)\, ds\, dr.$$

and hence

$$\rho_x(l) = \rho_x(0) - \frac{1}{D}\int_0^l F(s)\, ds$$

$$\rho(l) = \rho(0) + \rho_x(0)\, l - \frac{1}{D}\int_0^l \int_0^r F(s)\, ds\, dr.$$

The boundary conditions (86) and (87) lead to

$$\rho(0) = \frac{D\int_0^l F(s)\, ds + \alpha_- \int_0^l \int_0^r F(s)\, ds\, dr}{(\alpha_+ + \alpha_-)\, D + \alpha_+ \alpha_- l} + \frac{(D + \alpha_- l)\, \beta_+ \varphi_0 + D\beta_- \varphi_1}{(\alpha_+ + \alpha_-)\, D + \alpha_+ \alpha_- l}$$

$$\rho(l) = \frac{D\int_0^l F(s)\, ds + \alpha_+ \int_0^l \int_r^l F(s)\, ds\, dr}{(\alpha_+ + \alpha_-)\, D + \alpha_+ \alpha_- l} + \frac{(D + \alpha_+ l)\, \beta_- \varphi_1 + D\beta_+ \varphi_0}{(\alpha_+ + \alpha_-)\, D + \alpha_+ \alpha_- l}$$

If $F(x) \equiv F$, the above formulas reduce to (28) and (29). Relations (86) and (87) then give the expressions (30) and (31) for J_0^+ and J_1^-.

A.2. TE-Model with Evaporation

To incorporate the evaporation of terrace adatoms, we change (27) to the following form:

$$D\rho_{xx} - \frac{\rho}{\tau} = -F \tag{88}$$

$$J_j^+ = D\rho_x|_j^+ = \alpha_+(\rho_j^+ - \rho_e) - \beta_+(\varphi_j - \varphi_e) \tag{89}$$

$$J_j^- = -(D\rho_x|_j^-) = \alpha_-(\rho_j^- - \rho_e) - \beta_-(\varphi_j - \varphi_e) \tag{90}$$

$$\frac{d\varphi_j}{dt} = \dot{\varphi}_j = J_j^+ + J_j^- - \frac{v_j}{a^2} \tag{91}$$

$$v_j = a^2 k(\gamma\varphi_j - \delta) \tag{92}$$

where τ is the mean survival time for the terrace adatoms before they evaporate and ρ_e and φ_e are the equilibrium terrace and edge adatom densities.

We can solve for ρ by considering a similar cell problem as in Section A.1. By introducing the following notations:

$$l_j = x_{j+1} - x_j$$

$$\varepsilon_j = e^{l_j\eta}, \qquad \eta = \frac{1}{\sqrt{D\tau}}$$

$$L(l_j) = (D^2\eta^2 + \alpha_+\alpha_-)(\varepsilon_j - \varepsilon_j^{-1}) + D\eta(\alpha_+ + \alpha_-)(\varepsilon_j + \varepsilon_j^{-1})$$

we can write down the following expression for the rate of change of the edge adatom density:

$$\frac{d\varphi_j}{dt} + \frac{v_j}{a^2} = J_j^+ + J_j^- = (I) + (II) \tag{93}$$

where

$$\begin{aligned}
(I) &= \text{Contribution from } F \\
&= \left(\frac{D\eta(\varepsilon_j-\varepsilon_j^{-1})+\alpha_-(\varepsilon_j+\varepsilon_j^{-1}-2)}{\eta L(l_j)}\right)\alpha_+\left(F-\frac{\rho_e}{\tau}\right) && (94)\\
&\quad+\left(\frac{D\eta(\varepsilon_{j-1}-\varepsilon_{j-1}^{-1})+\alpha_+(\varepsilon_{j-1}+\varepsilon_{j-1}^{-1}-2)}{\eta L(l_{j-1})}\right)\alpha_-\left(F-\frac{\rho_e}{\tau}\right) && (95)\\
(II) &= \text{Contribution from } \varphi \\
&= 2\eta D\left(\frac{\alpha_+\beta_-+\alpha_-\beta_+}{2}\right)\left(\frac{\varphi_{j+1}-\varphi_j}{L(l_j)}-\frac{\varphi_j-\varphi_{j-1}}{L(l_{j-1})}\right) && (96)\\
&\quad+2\eta D\left(\frac{\alpha_+\beta_--\alpha_-\beta_+}{2}\right)\left(\frac{\varphi_{j+1}+\varphi_j}{L(l_j)}-\frac{\varphi_j+\varphi_{j-1}}{L(l_{j-1})}\right) && (97)\\
&\quad-\left(\frac{\alpha_-\beta_+(\varepsilon_j+\varepsilon_j^{-1}-2)+D\eta\beta_+(\varepsilon_j-\varepsilon_j^{-1})}{L(l_j)}\right)D\eta(\varphi_j-\varphi_e) && (98)\\
&\quad-\left(\frac{\alpha_+\beta_-(\varepsilon_{j-1}+\varepsilon_{j-1}^{-1}-2)+D\eta\beta_-(\varepsilon_{j-1}-\varepsilon_{j-1}^{-1})}{L(l_{j-1})}\right)D\eta(\varphi_j-\varphi_e) && (99)
\end{aligned}$$

It is clear that (94)–(97) resemble (32). The effect of evaporation is captured by (98) and (99). As a check of the above formulas, note that in the limit of no evaporation, i.e., as $\tau\to\infty$ (or $\eta\to 0$), we have

$$\varepsilon_j-\varepsilon^{-1}=2l_j\eta+O(l_j^3\eta^3) \tag{100}$$

$$\varepsilon_j+\varepsilon^{-1}-2=l_j^2\eta^2+O(l_j^4\eta^4) \tag{101}$$

$$L(l_j)=2\eta\{D(\alpha_++\alpha_-)+\alpha_+\alpha_-(l_j+O(l_j^2\eta))\} \tag{102}$$

From these, it follows that (94)–(99) converge to (32) (if we set φ_e to be zero).

To obtain the continuum limit of this model, we keep η *fixed* and consider the same scaling as in (38)– (46). Then we arrive at the following equation.[5]

---

[5] Here we follow the same notations as in (35) and (37). ρ_e and φ_e are set to zero.

Continuum Limit of TE-Model with Evaporation:

$$\frac{D\varphi}{Dt}+\frac{v}{a^2}=\frac{aF}{|h_x|}+a\partial_h(A(|h_x|)\,\partial_h\varphi)+2\left(\frac{\alpha_+\beta_- -\alpha_-\beta_+}{\alpha_+\beta_- +\alpha_-\beta_-}\right)\partial_h(A(|h_x|)\,\varphi)$$
$$-\left(\frac{aD\eta^2}{2}\right)\left(\frac{2(\beta_+ +\beta_-)\,D|h_x|+(\alpha_+\beta_- +\alpha_-\beta_+)\,a}{D(\alpha_+ +\alpha_-)\,|h_x|+\alpha_+\alpha_- a}\right)\frac{\varphi}{|h_x|} \tag{103}$$

Under our scaling, the deposition, diffusion and convective terms of (103) have the order of $O(a^2\beta)\,\varphi$ while the evaporation term is $O(a^2\eta^2\beta)\,\varphi$. So as $\eta\to 0$ (in the limit of no evaporation), (103) converges to (33).

A.3. Derivation of (79)—Averaging of Oscillatory Boundary Conditions

Here we briefly describe the derivation of (79) which is some kind of averaging of the oscillatory boundary conditions (72) and (73). It is a special case of the following result.

Let Ω^ε be a domain in R^2 with an oscillatory boundary $\partial\Omega^\varepsilon$ which is represented locally in graph by:

$$f_0(x)+\varepsilon f_1\left(x,\xi=\frac{x}{\varepsilon}\right) \tag{104}$$

where f_0 and f_1 are Lipschitz functions and f_1 is periodic in ξ with period one. Let u^ε be the solution of the following problem:

$$u_t^\varepsilon=\triangle u^\varepsilon,\qquad t>0,\, x\in\Omega^\varepsilon \tag{105}$$

$$\frac{\partial u^\varepsilon}{\partial n}+p(\hat{n}^\varepsilon)\,u^\varepsilon=0,\qquad t>0,\, x\in\partial\Omega^\varepsilon \tag{106}$$

$$u^\varepsilon=u_0^\varepsilon,\qquad t=0,\, x\in\Omega^\varepsilon \tag{107}$$

where $\hat{n}^\varepsilon$ is the outward normal of $\partial\Omega^\varepsilon$ and p is positive and continuous. Then u^ε will converge to u which is the solution of the following problem:

$$u_t=\triangle u,\qquad t>0,\, x\in\Omega \tag{108}$$

$$\frac{\partial u}{\partial n}+P(\hat{n})u=0,\qquad t>0,\, x\in\partial\Omega \tag{109}$$

$$u=u_0,\qquad t=0,\, x\in\Omega \tag{110}$$

where Ω is the limit of Ω^ε and P is some function which can be computed from p and f_1 (114).

Remark. The above result is worked out in refs. 8 and 3. By making use of H^2 estimates, they can even obtain the rate of convergence in H^1 norm. But here we will only consider H^1 estimates and use the fact that if a sequence u_n converges weakly to u in $H^1(\Omega)$, then the trace of u_n converges strongly in $L^2(\partial\Omega)$ to the trace of u on $\partial\Omega$. ▮

Sketch of Proof. For simplicity, we will assume that $\Omega \subset \Omega^\varepsilon$ for all $\varepsilon > 0$.

Using the weak formulation of the solution to (105)–(107), u^ε satisfies the following identity:

$$\int_0^1 \int_{\Omega^\varepsilon} u^\varepsilon \psi_t + \int_{\Omega^\varepsilon} u_0^\varepsilon \psi = \int_0^1 \int_{\Omega^\varepsilon} \langle \nabla u^\varepsilon, \nabla \psi \rangle + \int_0^1 \int_{\partial\Omega^\varepsilon} p(\hat{n}^\varepsilon)\, u^\varepsilon \psi \tag{111}$$

for all $\psi \in C^\infty([0, 1] \times \bar{\Omega}^\varepsilon)$ such that $\psi(1, \cdot) = 0$. By the usual H^1 energy estimates, it is easy to extract a subsequence such that

$$\begin{aligned} u^\varepsilon &\rightharpoonup u \qquad \text{weakly in} \quad H^1(\Omega) \\ u^\varepsilon &\to u \qquad \text{strongly in} \quad L^2(\partial\Omega) \end{aligned}$$

(By the uniqueness of the solution of the limiting problem (108)–(110), the convergence can be extended to the whole sequence.) Hence

$$\int_0^1 \int_{\Omega^\varepsilon} u^\varepsilon \psi_t \to \int_0^1 \int_{\Omega} u \psi_t$$

$$\int_{\Omega^\varepsilon} u_0^\varepsilon \psi \to \int_{\Omega} u_0 \psi$$

$$\int_0^1 \int_{\Omega^\varepsilon} \langle \nabla u^\varepsilon, \nabla \psi \rangle \to \int_0^1 \int_{\Omega} \langle \nabla u, \nabla \psi \rangle$$

For the last term of (111), we proceed as

$$\int_0^1 \int_{\partial\Omega^\varepsilon} p(\hat{n}^\varepsilon)\, u^\varepsilon \psi = \int_0^1 \int_{\partial\Omega^\varepsilon} p(\hat{n}^\varepsilon)(u^\varepsilon - u)\, \psi + \int_0^1 \int_{\partial\Omega^\varepsilon} p(\hat{n}^\varepsilon)\, u \psi \tag{112}$$

The first term on the right hand side tends to zero as u^ε converges strongly to u in $L^2(\partial\Omega)$. For the second term, it converges to

$$\int_0^1 \int_{\partial\Omega} P(\hat{n})\, u\psi \tag{113}$$

where $P(\hat{n})$ is derived in the following.

Suppose near $x \in \partial\Omega$, $\partial\Omega^\varepsilon$ is represented as a graph

$$\varepsilon f_1\left(x, \xi = \frac{x}{\varepsilon}\right)$$

so that the normal $\hat{n}$ of $\partial\Omega$ is along the y-axis. Since $\xi = \frac{x}{\varepsilon}$ is the fast variable, $P(\hat{n})$ can be given by the average of $p(\hat{n}^\varepsilon)$ over the *unit cell* of $\xi \in [0, 1]$:

$$P(n) = \int_0^1 p(f_\xi(\cdot, \xi))\sqrt{1 + f_\xi^2(\cdot, \xi)}\, d\xi. \tag{114}$$

So u satisfies the following identity:

$$\int_0^1 \int_\Omega u\psi_t + \int_\Omega u_0\psi = \int_0^1 \int_\Omega \langle \nabla u, \nabla\psi \rangle + \int_0^1 \int_{\partial\Omega} P(\hat{n})\, u\psi$$

which is the weak formulation of the solution to (108)–(110). ∎

In order to apply the above result to the case of (72) and (73), we consider the following piecewise linear function:

$$f_1(\cdot, \xi) = \begin{cases} (\tan\theta)\,\xi, & \xi \in [0, \cos^2\theta] \\ -(\cot\theta)(\xi - 1), & \xi \in [\cos^2\theta, 1] \end{cases}$$

$$p(\hat{n}_1) = \sigma$$

$$p(\hat{n}_2) = \lambda$$

where $\hat{n}_1$ and $\hat{n}_2$ are the normal vectors of f_1 for $\xi \in [0, \cos^2\theta]$ and $[\cos^2\theta, 1]$ respectively. Then

$$\begin{aligned} P(\hat{n}) &= \int_0^{\cos^2\theta} \sigma\sqrt{1 + \tan^2\theta}\, d\xi + \int_{\cos^2\theta}^1 \lambda\sqrt{1 + \cot^2\theta}\, d\xi \\ &= \sigma\cos\theta + \lambda\sin\theta \end{aligned}$$

which is exactly (79).

A.4. Multiple Species

In this section, we introduce a model of multiple species in which two types of deposition adatoms (species A and B) land on the interface and interact to form a third species C which is then incorporated into the crystal. This is the simplest example of nontrivial chemistry.

We consider the **TE-Model** with vapor diffusion for the species A and B:

$$\frac{\partial \Gamma^A}{\partial t} = D_b^A \triangle \Gamma^A = D_b^A(\partial_x^2 \Gamma^A + \partial_z^2 \Gamma^A)$$

$$\frac{\partial \Gamma^B}{\partial t} = D_b^B \triangle \Gamma^B = D_b^B(\partial_x^2 \Gamma^B + \partial_z^2 \Gamma^B)$$

etc. (Note that the diffusion constants and attachment/detachment rates might depend on the species A and B.) In the present case, φ_j^A and φ_j^B are lost *not* to the film but to the formation of the new species C. So (77) and (11) need to be modified as follows:

$$\frac{d\varphi_j^S}{dt} = J_j^{S+} + J_j^{S-} + D_b^S \int_{z_j}^{z_{j+1}} \frac{\partial \Gamma^S}{\partial x}(x_j, z, t)\, dz - \frac{d\varphi_j^C}{dt}, \qquad (S = A, B) \tag{115}$$

$$\frac{d\varphi_j^C}{dt} = \Lambda \varphi_j^A \varphi_j^B \tag{116}$$

$$v_j = a^2 k(\gamma \varphi_j^C - \delta) \tag{117}$$

where φ^C is the edge adatom density of species C and Λ is the reaction rate.

Now the set of Eqs. (70)–(76) (one for each of A and B) and (117)–(117) completely determines the evolution of the variables $\Gamma^{A,B}$, $\rho^{A,B}$, $\varphi^{A,B,C}$ and v_j.

Remark. In the present model, we only consider the reactions at the steps. Of course, we can easily modify the equations to allow reactions on the terraces and even in the vapor state. ▮

A.4.1. Continuum Limit of TE-Model for Multiple Species

Following the same notations as in Section 6.1, we can write down the continuum limit of the present model for multiple species.

The adatom densities Γ^A, Γ^B solve the following equation ($S = A$ or B):

$$\frac{\partial \Gamma^S}{\partial t} = D_b^S \triangle \Gamma^S = D_b^S(\partial_x^2 \Gamma^S + \partial_z^2 \Gamma^S) \qquad \text{for} \quad z > h(x,t) \tag{118}$$

with the boundary conditions

$$D_b^S \frac{\partial \Gamma^S}{\partial n} = -(\sigma^S \cos\theta + \lambda^S \sin\theta)\, \Gamma^S \qquad \text{at} \quad z = h(x,t) \tag{119}$$

$$\Gamma^S(x, +\infty, t) = F^S. \tag{120}$$

Here n and θ are defined in the same way as in (83) and (84).

The edge adatom densities (φ^A, φ^B) solve the following equation:

$$\frac{D\varphi^S}{Dt} = a\Gamma^S(x, h(x,t))\left(\lambda^S + \frac{\sigma^S}{|h_x|}\right) + a\partial_h(A^S(|h_x|)\,\partial_h \varphi^S) + Q^S \partial_h(A(|h_x|)\,\varphi) - \frac{d\varphi^C}{dt}$$

(1

where

$$Q^S = \frac{\alpha_+^S \beta_-^S - \alpha_-^S \beta_+^S}{\alpha_+^S \beta_-^S + \alpha_-^S \beta_+^S} \tag{122}$$

and $A^S(|h_x|)$ has the same form as (36) but with the constants D_ρ^S, $\alpha_\pm^S$ and $\beta_\pm^S$ which might depend on the species A or B.

The rate of change of φ^C is given by

$$\frac{d\varphi^C}{dt} = \Lambda \varphi^A \varphi^B. \tag{123}$$

Finally, we have the similar conditions for the step velocity and the interfacial growth:

$$v = a^2 k(\gamma \varphi^C - \delta), \qquad h_t = v\,|h_x|. \tag{124}$$

Remark. The derivation of the continuum limit is very similar to that of the model with vapor diffusion (Section 6.1). Note that φ_j^A, φ_j^B can be shown to converge *strongly* to φ^A, φ^B. Hence we can write down (123) at the continuum level. ▮

ACKNOWLEDGMENTS

The authors would like to thank Bob Kohn and Tim Schulze for very helpful discussions. This work was partially supported by NSF and DARPA through the VIP program. The second author would also like to acknowledge support from the New York University Research Challenge Fund.

REFERENCES

1. I. Bena, C. Misbah, and A. Valance, Nonlinear evolution of a terrace edge during step-flow growth, *Phys. Rev. B* **47**:7408 (1993).
2. W. K. Burton, N. Cabrera, and F. C. Frank, The growth of crystals and the equilibrium structure of their surfaces, *Phil. Trans. Roy. Soc. London Ser. A* **243**:299 (1951).
3. G. Chechkin, A. Friedman, and A. Piatnitski, The boundary-value problem in domains with very rapidly oscillating boundary, *J. Math. Anal. Appl.* **231**:213–234 (1999).
4. R. E. W. Caflisch, M. F. Gyure, B. Merriman, and C. Ratsch, Kinetic model for a step edge in epitaxial growth, *Phys. Rev. E* **59**:6879–6887 (1999).
5. S. A. Chalmers, J. Y. Tsao, and A. C. Gossard, Lateral motion of terrace width distributions during step-flow growth, *Appl. Phys. Lett.* **61**:645–647 (1992).
6. A. A. Chernov, *Modern Crystallography III—Crystal Growth* (Springer-Verlag, 1984).
7. S. F. Edwards and D. R. Wilkinson, The surface statistics of a granular aggregate, *Proc. Roy. Soc. London A* **381**:17–31 (1982).
8. A. Friedman, B. Hu, and Y. Liu, A boundary value problem for the Poisson equation with multi-scale oscillating boundary, *J. Diff. Eqn.* **137**:54–93 (1997).
9. N. Israeli and D. Kandel, Profile scaling in decay of nanostructures, *Phys. Rev. Lett.* **80**:3300–3303 (1998).
10. M. Kardar, G. Parisi, and Y. C. Zhang, Dynamic scaling of growing interfaces, *Phys. Rev. Lett.* **56**:889–892 (1986).
11. J. Krug, On the shape of wedding cakes, *J. Stat. Phys.* **87**:505–518 (1997).
12. J. S. Langer, Instabilities and pattern formation in crystal growth, *Rev. Modern Phys.* **52**(1):1–28 (1980).
13. W. W. Mullins, Theory of thermal grooving, *J. Appl. Phys.* **28**:333–339 (1957).
14. W. W. Mullins and R. F. Sekerka, Morphological stability of a particle growing by diffusion or heat flow, *J. Appl. Phys.* **34**(2):323–329 (1963).
15. W. W. Mullins and R. F. Sekerka, Stability of a planar interface during solidification of a dilute binary alloy, *J. Appl. Phys.* **35**:444–451 (1964).
16. M. Ozdemir and A. Zangwill, Morphological equilibration of a corrugated crystalline surface, *Phys. Rev. B* **42**:5013–5024 (1990).
17. P. Pelcé, ed., *Dynamics of Curved Fronts* (Academic Press, Boston, 1988).
18. A. Pimpinelli and J. Villain, *Physics of Crystal Growth* (Cambridge University Press, 1998).
19. P. Politi and J. Villain, Ehrlich–Schwoebel instability in molecular-beam epitaxy: A minimal model, *Phys. Rev. B* **54**:5114–5129 (1996).
20. O. Pierre-Louis, C. Misbah, Y. Saito, J. Krug, and P. Politi, New nonlinear evolution equation for steps during molecular beam epitaxy on vicinal surfaces, *Phys. Rev. Lett.* **80**:4221 (1998).
21. T. Schulze and W. E, A continuum model for the growth of epitaxial films, *J. Crystal Growth*, to appear.

22. P. Šmilauer and D. D. Vvedensky, Coarsening and slope evolution during unstable epitaxial growth, *Phys. Rev. B* **52**:14263–14272 (1995).
23. H. Spohn, Surface dynamics below the roughening transition, *J. de Physique* **3**:69 (1996).
24. S. Tanaka, N. C. Bartelt, C. C. Umbach, R. M. Tromp, and J. M. Blakely, Step permeability and the relaxation of biperiodic gratings in Si(001), *Phys. Rev. Lett.* **78**:3342–3345 (1997).
25. J. Y. Tsao, *Fundamentals of Molecular Beam Epitaxy* (Boston, Academic Press, 1988).
26. J. Villain, Continuum models of crystal growth from atomic beams with and without desorption, *J. Phys. I* **1**:19–42 (1991).
27. D. D. Vvedensky, A. Zangwill, C. N. Luse, and M. R. Wilby, Stochastic equations of motions for epitaxial growth, *Phys. Rev. E* **48**:852–862 (1993).
28. Y. Xiang, Ph.D. thesis, New York University, in preparation.